

RESEARCH

Open Access



Asian sand dust exacerbates airway inflammation in a mouse model of asthma

Se-Jin Lee¹, So-Won Pak¹, Woong-Il Kim¹, Sin-Hyang Park¹, Young-Kwon Cho², Tae-Won Kim³, Je-Won Ko³, Joong-Sun Kim¹, Jong-Choon Kim¹, In-Hyeon Kim⁴, Sung-Hwan Kim^{4*} and In-Sik Shin^{1*} 

Abstract

Background Asian sand dust (ASD), generated from the deserts of China and Mongolia, mainly affects the human health of several countries in Northeast Asia including China, Korea, and Japan. In this study, we investigated the toxic effects of ASD on respiratory tract and explored the effects of ASD exposure on allergic asthma using ovalbumin-induced asthma model. C57BL/6 male mice were used for both the toxicity and allergic asthma studies. ASD (10, 20, and 40 mg/kg) was administered intranasally on days 1, 3, and 5. For allergic asthma, mice were sensitized with OVA (20 µg/mouse) and aluminum hydroxide (2 mg) on days 1 and 15, followed by OVA inhalation (1%, w/v) on days 22, 24, and 26, with subsequent ASD instillation on days 21, 23, and 25.

Results ASD exposure showed the elevation of respiratory inflammation including inflammatory cell infiltration, cytokine production, and mucus secretion with the increase in phosphorylated (p)-nuclear factor-kappa B (NF-κB) p65 expression. In addition, ASD exposure to asthma model significantly increased airway responsiveness, inflammatory cell count and mucus secretion with the elevation of cytokines and immunoglobulin E, which were accompanied with the increases in p-NF-κB p65, p-p38 and cyclooxygenase 2 (COX2).

Conclusions Therefore, ASD exposure induces respiratory inflammation and aggravates the progression of allergic asthma, which was closely associated with the phosphorylation of NF-κB. Respiratory exposure to ASD causes inflammation, upregulation of cytokines, p-NF-κB, and COX2, which can exacerbate asthma.

Keywords Asian sand dust, Pulmonary toxicity, Allergic asthma, Nuclear factor-kappa B

Background

Asian sand dust (ASD) is an air-pollutant from the deserts of China and Mongolia [1]. ASD is commonly called yellow dust or China dust, and mainly affects Northeast Asia including China, Korea, and Japan during the spring and autumn [2]. Additionally, since the number of patients with respiratory disease increases during these seasons due to temperature changes and decreased immunity, exposure to ASD may lead to an increase in patients with respiratory diseases and worsening of underlying diseases. Because the use of masks is recommended during these corresponding seasons, normal activities of people are complicated [3]. In addition,

*Correspondence:

Sung-Hwan Kim
sunghwan.kim@kitox.re.kr
In-Sik Shin
dvmmk79@gmail.com

¹College of Veterinary Medicine and BK21 FOUR Program, Chonnam National University, 77 Yong-bong-ro, Buk-gu, Gwangju 61186, Republic of Korea

²College of Health Sciences, Cheongju University, 298 Daesung-ro, Sangdang-gu, Cheongju-si, Chungbuk 28503, Republic of Korea

³BK21 FOUR Program, College of Veterinary Medicine, Chungnam National University, 99 Daehak-ro, Daejeon 34134, Republic of Korea

⁴Jeonbuk Branch, Korea Institute of Toxicology (KIT), Jeongeup-si Jeonbuk 53212, Republic of Korea



© The Author(s) 2025. **Open Access** This article is licensed under a Creative Commons Attribution 4.0 International License, which permits use, sharing, adaptation, distribution and reproduction in any medium or format, as long as you give appropriate credit to the original author(s) and the source, provide a link to the Creative Commons licence, and indicate if changes were made. The images or other third party material in this article are included in the article's Creative Commons licence, unless indicated otherwise in a credit line to the material. If material is not included in the article's Creative Commons licence and your intended use is not permitted by statutory regulation or exceeds the permitted use, you will need to obtain permission directly from the copyright holder. To view a copy of this licence, visit <http://creativecommons.org/licenses/by/4.0/>. The Creative Commons Public Domain Dedication waiver (<http://creativecommons.org/publicdomain/zero/1.0/>) applies to the data made available in this article, unless otherwise stated in a credit line to the data.

as desertification and industrialization progress, various harmful substances generated therefrom have been included in ASD, threatening human health further. According to a recent study, ASD has increased particulate matter (PM)₁₀ and PM_{2.5} levels and includes PM-bound trace metals such as aluminum (Al), arsenic (As), calcium (Ca), copper (Cu), Iron (Fe), nickel (Ni), lead (Pb), and Zinc (Zn) and various bacteria, which increase the occurrence of cardiovascular and respiratory diseases [4]. Furthermore, because ASD contains a lot of silica, there is a risk of causing silicosis, which is proven by the occurrence of silicosis in artificial stone workers who are at high risk of exposure to silica dust [5]. Therefore, ASD is regarded as an important social issue that threatens human health. This is not limited to Korea, as it is also considered an important social problem in China and Japan, which are affected by ASD via air currents [6, 7].

Allergic asthma is regarded as a complex inflammatory disorder of the pulmonary system that has features such as airway hypersensitivity, eosinophilia, and mucus production, leading to several clinical symptoms such as chest tightness, cough, dyspnea, and wheezing [8]. It is caused by exposure to allergens, which induce asthmatic characteristics via inflammatory cytokines such as interleukin (IL)-4, -5, and -13 [9]. During the progression of allergic asthma, exposure to other exogenous stimuli exacerbates the symptoms of allergic asthma, and recently, as ASD has increased, the incidence of allergic asthma has increased and the condition of patients with allergic asthma has worsened [4].

Various signaling pathways related to inflammatory responses are associated with the pathogenesis of allergic asthma. Regarding signaling pathways, nuclear factor-kappa B (NF- κ B) acts as a crucial transcription factor that produces various inflammatory mediators and is related to the pathogenesis of various diseases [10]. The most abundant form of NF- κ B is the p50/p65 dimer, and the phosphorylation of p65 by pathologic stimuli plays a pivotal role in several chronic inflammatory conditions [11]. In the progression of allergic asthma, elevated phosphorylated (p)-NF- κ B expression induces the releases of inflammatory mediators including cytokines, cyclooxygenase 2 (COX2) and matrix metalloproteinases, which eventually accelerate airway inflammation. In particular, tumor necrosis factor (TNF)- α and IL-6 induce acute inflammatory responses by participating in the recruitment and activation of inflammatory cells [12]. When respiratory system is exposed to specific irritants, the production of TNF- α and IL-6 increases and the resulting inflammatory response in lung tissue is significantly aggravated [13]. Moreover, in asthma, TNF- α interacts with other cytokines, leading to the recruitment of inflammatory cells to the airways and contributing to airway remodeling [14]. Thus, NF- κ B is regarded as a major

target for allergic asthma and an indicator of asthma severity [13].

Therefore, we investigated the pulmonary toxicity induced by ASD exposure and then evaluated its aggravative effect on allergic asthma caused by ovalbumin (OVA). Furthermore, to identify the toxic mechanism of ASD, we performed a biochemical analysis focusing on NF- κ B.

Methods

Asian sand dust (ASD)

ASD (POWDER TECHNOLOGY Inc., Arden Hills, MN) is a 50/50 mixture of JIS Z8901 Class 8 test dust and naturally occurring silicon dioxide. The morphology of ASD was determined using transmission electron microscopy (TEM, JEM-2100 F, JEOL, Tokyo, Japan), and the primary size of ASD was evaluated using scanning electron microscopy (SEM, Zeiss Gemini500, Carl Zeiss Meditec AG, Jena, Germany), and subsequently measuring the sizes of 200 particles using ImageJ software. The purity of ASD was evaluated using energy-dispersive X-ray spectroscopy (Oxford Instrument, Abingdon, UK). Zeta potential and hydrodynamic size were measured using a dynamic light scattering instrument (ELSZneo, Otsuka Electronics, Tokyo, Japan).

Experimental design

C57BL/6 male mice (6 weeks old, 18–20 g) without specific pathogens were purchased from SAMTAKO (Osan, Republic of Korea). To establish a toxicity study of ASD, 28 animals were randomly designed into four experimental groups (each group, $n=7$) as follows: NC (normal control), and ASD 10, 20, and 40 (10, 20, and 40 mg/kg of ASD, respectively) (Fig. 1A). ASD was administered by intranasal instillation on days 1, 3, and 5. Exposure dose of ASD was determined according to previous study [2]. The instillation dose of ASD (40 mg/kg) was 5.3 times higher than the national air quality standard for suspended PM, as PM levels during ASD events in Korea often exceed 150 $\mu\text{g}/\text{m}^3$ [15].

To investigate the deteriorative effects of ASD exposure on allergic asthma, mice were designated into 5 groups (each group, $n=7$) as follows: NC (normal control), OVA (asthma model), and ASD10, 20, and 40+OVA (10, 20, and 40 mg/kg of ASD exposure+asthma model). As shown in Fig. 1B, the protocol to induce asthma was conducted according to previous studies [8, 12, 16]. The animals received OVA (A5503, Sigma-Aldrich, St. Louis, MO) sensitization (20 $\mu\text{g}/\text{mouse}$ of OVA + 2 mg of aluminum hydroxide (77161, Thermo Fisher, San Diego, CA)) via intraperitoneal administration on days 1 and 15. OVA (1%, w/v, in phosphate-buffered saline (PBS)) inhalation was performed once a day for 1 h on days 22, 24, and 26 using a nebulizer (Omron, Tokyo, Japan). The intranasal

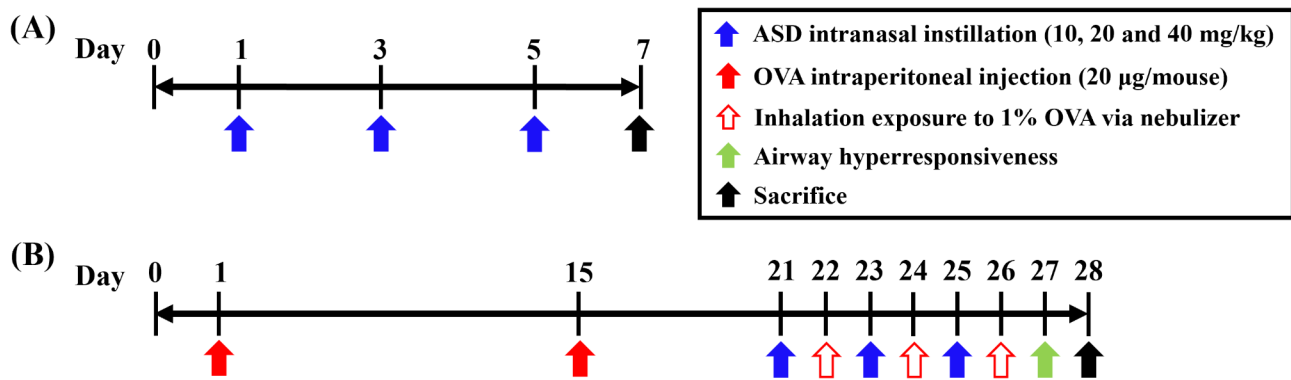


Fig. 1 Experimental procedures of pulmonary toxicity and allergic asthma. **(A)** Experimental procedure for pulmonary toxicity, **(B)** experimental procedure for allergic asthma

instillation of ASD (10, 20, and 40 mg/kg) was performed once a day on days 21, 23, and 25. Airway hyperresponsiveness (AHR) was performed 24 h after the final OVA inhalation. AHR of the mice was assessed using single-frequency forced oscillation with Flexivent (SCIREQ, Montreal, Canada). Under anesthesia with alfaxalone (Jurox Pty Ltd., Hunter Valley, Australia), a tracheostomy was performed to insert a cannula connected to a nebulizer containing PBS or methacholine (0, 10, 20, and 40 mg/mL; A2251, Sigma-Aldrich). The sequence of making measurements, nebulizing with methacholine solution for 10 s, recording airway resistance for 1 min, and refreshing for 2 min, was automatically repeated.

The animals used in toxicity and asthma experiments were sacrificed on days 7 and 28, respectively. Bronchoalveolar lavage fluid (BALF) was collected 48 h after the final challenge. Mice were anesthetized via intraperitoneal injection of alfaxalone (Jurox Pty Ltd.) and underwent tracheostomy. The lungs were lavaged twice with 0.7 mL of ice-cold PBS, and the obtained BALF samples were then centrifuged. The separated supernatants were used to measure inflammatory cytokines. BALF pellets were resuspended with PBS and then the number of total inflammatory cells was measured by an automated cell counter (Thermo Fisher). In addition, resuspended BALF pellets were attached to glass slides using cytospin (Hanil Science Industrial, Seoul, Korea), which were stained with Diff-Quik solution (Sysmax, Kobe, Japan) and representative pictures per slide were captured by microscopy using a slide scanner (Motic, Hong Kong). We counted inflammatory cells including neutrophils, macrophages, eosinophils, and lymphocytes, which were applied to total inflammatory cell counts obtained from the cell counter to determine the number of differential inflammatory cell counts.

Approval of animal studies was in accordance with the ethical guidelines and regulations established by the Institutional Animal Care and Use Committee of Chonnam National University (IACUC) carried out under

approval numbers CNU IACUC-YB-R-2020-93 and CNU IACUC-YB-R-2021-36.

Analysis of pathophysiological mediators in BALF and serum

BALF supernatant was used to determine the release of inflammatory cytokines including TNF- α , IL-4, -6, and -13 using commercial enzyme-linked immunosorbent assay (ELISA) kit (R&D Systems, Minneapolis, MN). Blood sample was drawn from the caudal vena cava and centrifuged to collect serum, which was used to evaluate OVA-specific immunoglobulin (Ig) E using commercial ELISA kit (BioLegend, San Diego, CA).

Histopathological examination

The left pulmonary lobes from each mouse were fixed with 10% neutralized formalin (Sigma-Aldrich) and embedded in paraffin to make a paraffin block for the evaluation of histological alterations. Then, paraffin blocks were cut to a 4 μ m thickness and attached to glass slides. For the evaluation of histological alterations including inflammatory cell accumulation and mucus production, the slides were stained with hematoxylin and eosin (Sigma-Aldrich) or periodic acid Schiff's solution (Sigma-Aldrich). Furthermore, to determine the expression of p-NF- κ B p65 in pulmonary tissues, we performed immunohistochemistry using commercial kits (Vector Laboratories, Burlingame, CA). The primary antibody for p-NF- κ B p65 (MA5-15160, Thermo Fisher) was diluted at a ratio of 1:200, and the procedure was conducted according to the protocol provided by the manufacturer. The representative figures for histological examination were obtained using a slide scanner (Motic) and the quantification of pulmonary inflammatory responses, mucus secretion, and protein expression were carried out using an IMT i-Solution, as an image analyzer (IMT i-Solution Inc., Vancouver, BC, Canada). In quantitative analysis of inflammation, we evaluated inflammatory response for total area (captured on 200 \times magnification).

In quantitative analysis of mucus secretion, we evaluated mucus secretion for bronchial area. Quantitative value was expressed as percent (% inflammation or mucus secretion area vs. arranged area).

Western blotting

Right pulmonary lobes were homogenized in a tissue lysis/extraction reagent (1/10 w/v; Sigma-Aldrich) contained with a protease inhibitor (P8340, Sigma-Aldrich). The protein quantification for each sample was performed using Bradford reagent (5000205, Bio-Rad, Hercules, CA) according to the manufacturer's instructions. A total of 30 μg of cellular protein was quantified and then separated using electrophoresis. The separated proteins were transferred to a nitrocellulose membrane, followed by incubation in blocking solution (5% skim milk). After removing the blocking solution, the membrane was incubated with the primary antibody at 4 $^{\circ}\text{C}$ overnight. After removing the primary antibody, the membrane was washed three times with Tris-buffered saline containing Tween 20 (TBST). Following the removal of the Tris buffer, the membrane was incubated with the secondary antibody, goat anti-rabbit IgG (H+L) HRP (1:10,000 dilution; 31460, Thermo Fisher), at room temperature for 30 min. After removing the secondary antibody, the membrane was washed five times with TBST for 15 min each. The quantification of protein expression was performed using Chemi-Doc (Bio-Rad). The primary antibodies used were as follows: p-p38 (1:1000; 4511, Cell

signaling, Danvers, MA), p-NF- κB p65 (1:1000; MA5-15160, Thermo Fisher), β -actin (1:1000; 4967, Cell Signaling), and COX2 (1:1000; ab15191, Abcam, Waltham, MA).

Statistical analysis

The data are expressed as the mean \pm standard deviation. Statistical analysis was performed using analysis of variance followed by Dunnett's adjustment using GraphPad Prism 5 (GraphPad Software, CA). A p-value < 0.05 was regarded as statistically significant.

Results

Characteristic analysis of ASD

The morphology and size of ASD were measured by SEM and TEM analysis (Fig. 2A, B). The component segments of ASD were investigated by TEM analysis (Fig. 2C). ASD morphology was mostly spherical and the primary size of ASD was 292 ± 186.2 nm. The composition of ASD consisted of 48.82% O, 43.4% Si, 4.73% Al, 2.15% Fe, 0.36% Mg, 0.3% Ti, and 0.24% Ca (Fig. 2D). As a result of measuring the zeta-potential of ASD, the average negative zeta potential was -32.48 mV (Fig. 2E). The average diameter of ASD in water was 1807.2 nm (Fig. 2F).

ASD exposure increased the inflammatory indices in the BALF of mice

ASD groups had significantly elevated the number of inflammatory cells in the BALF compared with the NC

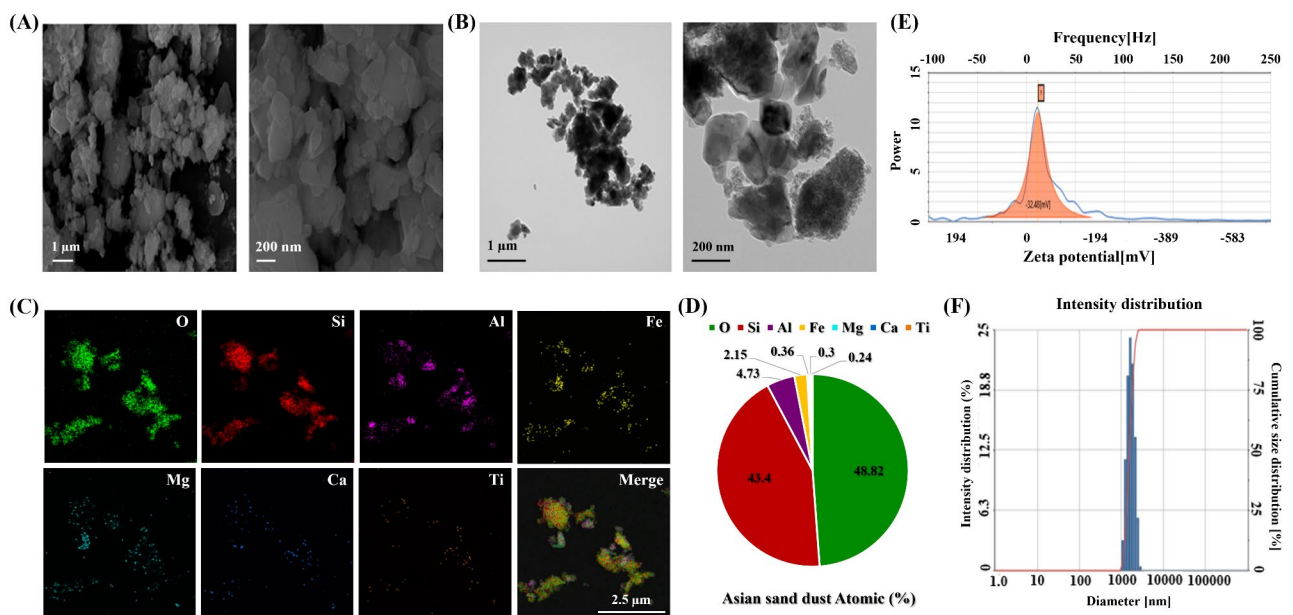


Fig. 2 Characteristic of Asian Sand Dust (ASD). (A) Figure of Scanning electron microscopy (SEM) for ASD, (B) figure of Transmission electron microscopy (TEM) for ASD, (C) representative figure of ASD composition analyzed by X-ray spectroscopy on SEM images, (D) quantitative analysis of ASD composition, (E) average zeta potential of ASD in water, and (F) average particle size of ASD in water

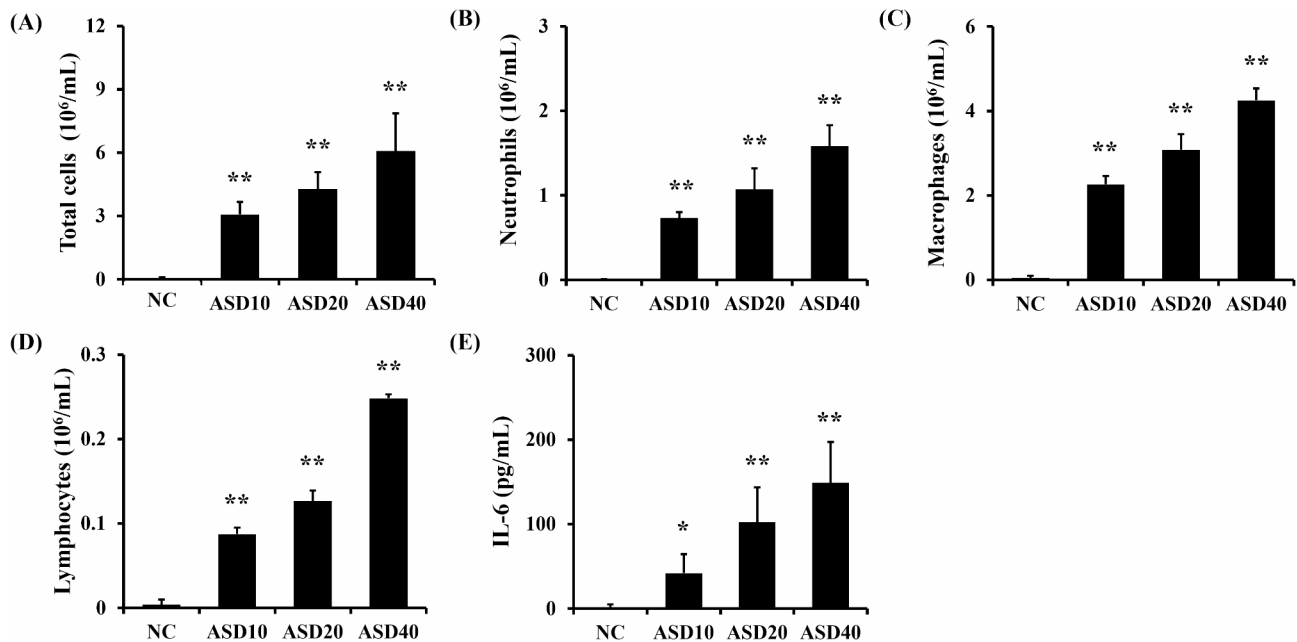


Fig. 3 Effects of ASD on inflammatory cell counts and inflammatory cytokines in Bronchoalveolar lavage fluid (BALF). **(A)** Total cells, **(B)** macrophages, **(C)** neutrophils, **(D)** lymphocytes, and **(E)** Interleukin (IL)-6 levels. Normal control (NC), PBS intranasal instillation: ASD10, 20, and 40, ASD (10, 20, and 40 mg/kg, respectively) intranasal instillation ($n=7$). **, versus NC, $p < 0.05$ and < 0.01 , respectively

group, which was dose-dependent (Fig. 3A). In particular, the counts of macrophages and neutrophils in the BALF was considerably elevated in comparison to those of the NC group (Fig. 3B, C). In addition, the number of lymphocytes was markedly elevated by ASD exposure in a dose-dependent manner (Fig. 3D). The releases of IL-6 in the BALF were meaningfully increased by ASD exposure in dose-dependent manner (Fig. 3E).

ASD exposure increased pulmonary inflammation and p-NF- κ B expression in pulmonary tissues

ASD groups had a considerably increased infiltration of inflammatory cells into pulmonary tissues compared with the NC group, which was dose-dependent (Fig. 4A, C). Similar to the results of inflammatory responses in lung tissues, p-NF- κ B p65 expression was markedly increased by ASD exposure, which was dose-dependent (Fig. 4B, D). Western blotting showed that ASD groups had significantly elevated expressions of p-p38, p-NF- κ B p65, and COX2, which was dose-dependent (Fig. 4E, F).

ASD exposure elevated the pathophysiological index in the BALF and serum from OVA-inhaled mice

The OVA group had a considerably elevated the number of inflammatory cells in the BALF compared with those of the NC group (Fig. 5A–E). However, ASD + OVA groups elevated the number of inflammatory cells in the BALF compared with those of the OVA group according to the increase in dose of ASD, and significant differences were detected in the ASD40 + OVA group.

The releases of TNF- α , IL-4, -6, and -13 were obviously elevated in the OVA group in comparison to those of the NC group (Fig. 5F–I). ASD + OVA group increased inflammatory cytokines in the BALF compared with those of the OVA group, and considerable differences in the releases of IL-4, -6, and -13 were seen in the ASD + OVA groups. Consistent with the results of cytokines, the release of OVA-specific IgE was considerably elevated in the OVA group in comparison to the NC group. Moreover, ASD + OVA group significantly elevated in comparison to the OVA group (Fig. 5J).

ASD exposure increased AHR and mucus production in OVA-inhaled mice

The OVA group had markedly elevated AHR compared with the NC group along with an increasing dose of methacholine (Fig. 6A). ASD + OVA group increased in comparison to those of the OVA group, especially in the ASD40 + OVA group. In addition, the OVA group had considerably elevated mucus production compared with the NC group (Fig. 6B). ASD + OVA group considerably elevated mucus production in comparison to the OVA group.

ASD exposure elevated airway inflammation and p-NF- κ B expression in pulmonary tissues from OVA-inhaled mice

The OVA group had a markedly increased accumulation of inflammatory cells into pulmonary tissues compared with the NC group (Fig. 7A, C). ASD + OVA group considerably increased the accumulation of inflammatory

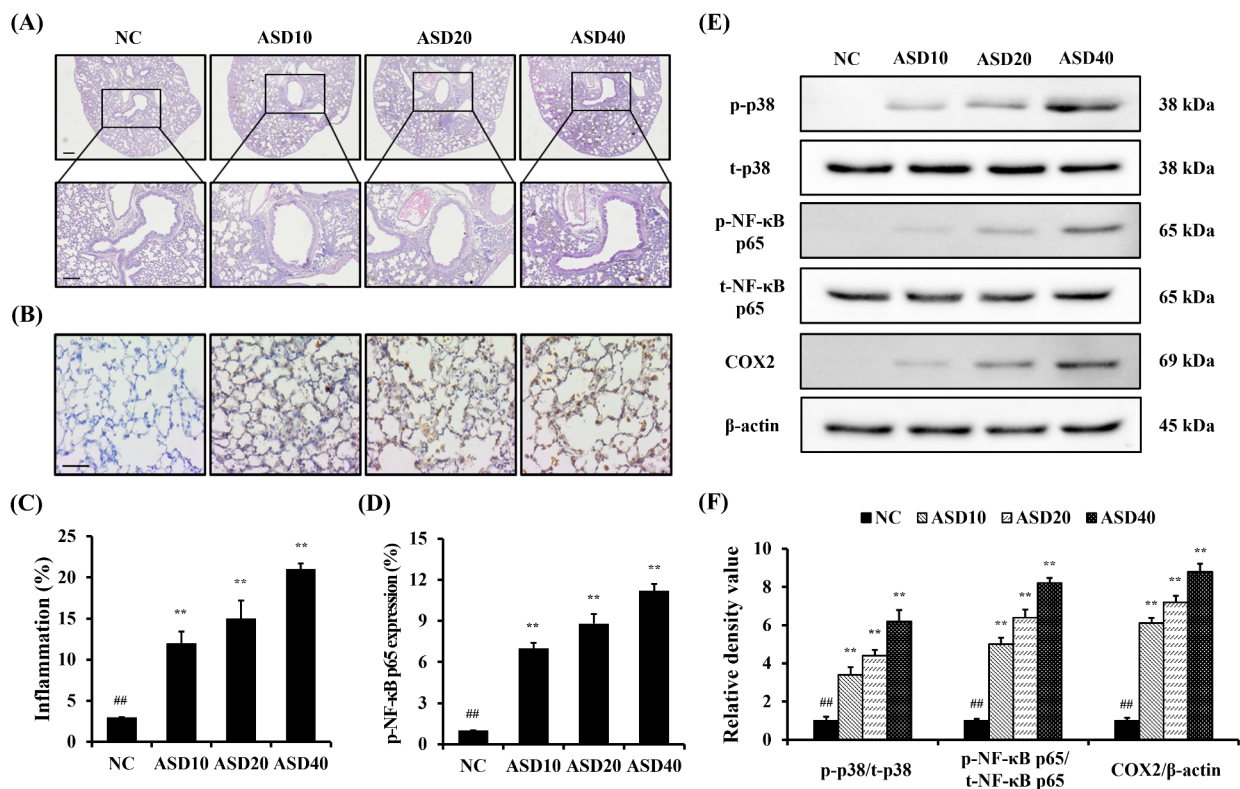


Fig. 4 Effects of ASD on inflammatory responses and p-NF-κB expression in pulmonary tissues. **(A)** Representative figure of Hematoxylin & Eosin (H&E) staining, **(B)** representative figure for Immunohistochemical (IHC) (p-NF-κB p65), **(C)** quantitative analysis of inflammation, **(D)** quantitative analysis of p-NF-κB p65 expression, **(E)** representative figure for Western blot, **(F)** Relative density value of each protein. NC, PBS intranasal instillation; ASD10, 20, and 40, ASD (10, 20, and 40 mg/kg, respectively) intranasal instillation ($n=7$). **, versus NC, $p<0.01$

cells into pulmonary tissues compared with the OVA group. Consistently, p-NF-κB p65 expression was obviously elevated in the OVA group compared with the NC group (Fig. 7B, D). ASD+OVA group considerably elevated p-NF-κB p65 expression in comparison to the OVA group. The OVA group had obviously elevated expressions of p-p38 and p-NF-κB p65 in comparison to the NC group (Fig. 7E, F). ASD+OVA group considerably elevated the expression of p-p38 and p-NF-κB p65 in comparison to the OVA group. Additionally, COX2 expression was obviously elevated in the OVA group compared with the NC group. But, ASD+OVA group increased COX2 expression compared with the OVA group.

Discussion

The risk of ASD is increasing every year, and in particular, as various harmful components such as chemicals, nanoparticles, bacterial toxins, and allergens are included, the possibility of threatening human health is very high [17]. In Northeast Asia, where ASD mainly occurs, the prevalence of various diseases caused by ASD is continuously increasing [18]. Particularly, exposure to ASD has been involved in an elevation of the occurrence

of respiratory diseases or aggravation of respiratory diseases [19]. In present study, we investigated the respiratory toxicity of ASD and explored the effects of its exposure on underlying respiratory disease using OVA-inhaled allergic asthma. The exposure to ASD markedly increased inflammatory cells and cytokines in the BALF, which was accompanied by pulmonary inflammation with the phosphorylation of NF-κB expression. In addition, ASD exposure elevated AHR, cytokines, the number of inflammatory cells, and OVA-specific IgE in OVA-inhaled mice, which was accompanied by the exacerbation of histopathological alterations of asthma including pulmonary inflammatory responses and mucus production. These responses were associated with the increase in p-NF-κB p65 expression as well as toxicity of ASD.

In this study, the particle size distribution of ASD, with a primary size of 292 ± 186.2 nm and a predominantly spherical morphology, places it within the inhalable range, facilitating its suspension in the air and potential to reach the lungs upon inhalation [20]. Particles with a diameter smaller than $10 \mu\text{m}$ can reach the lungs, and those smaller than $1 \mu\text{m}$ have the potential to enter the bloodstream, triggering immune responses. ASD consists primarily of fine and ultrafine particles, with a significant

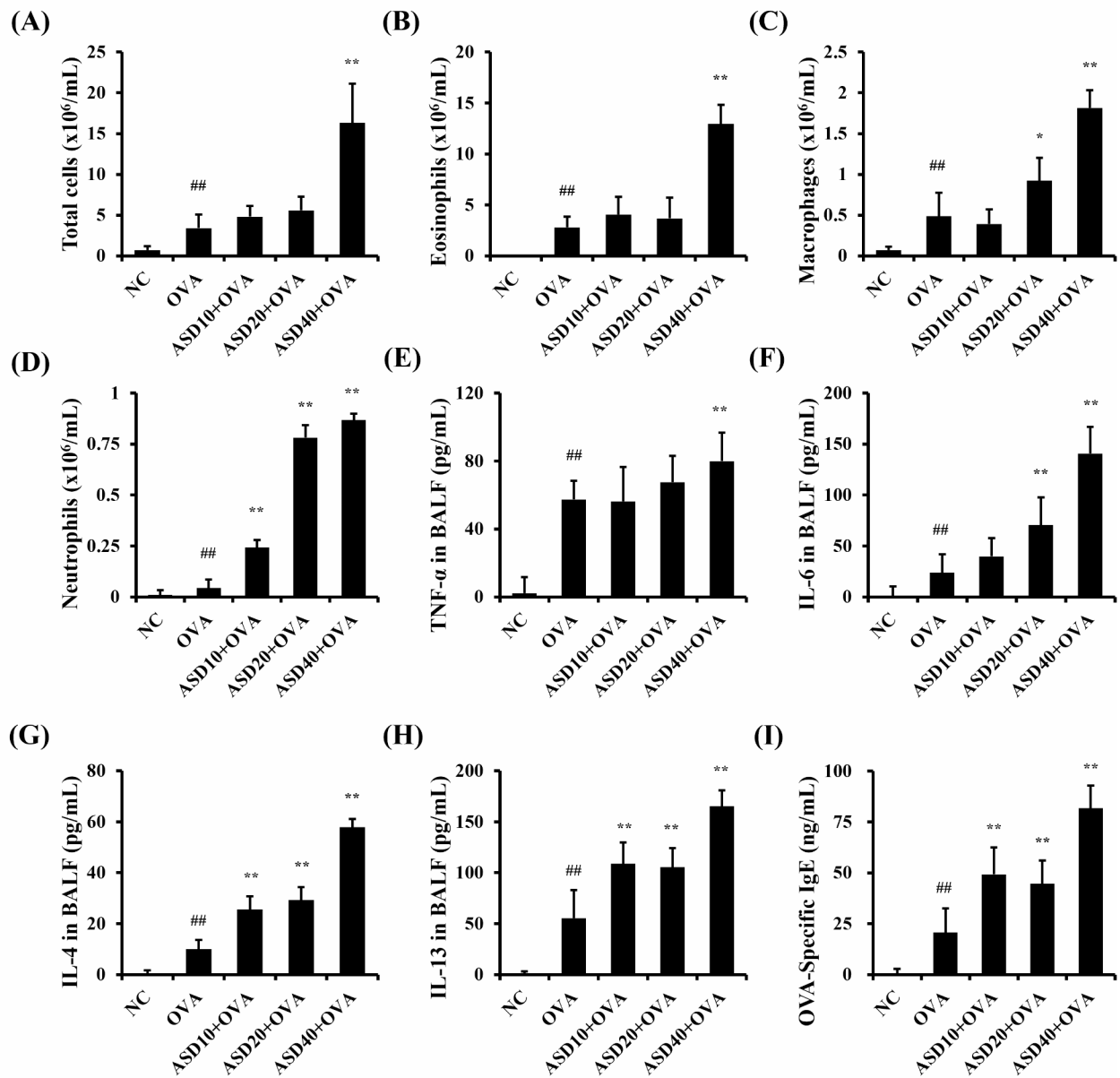


Fig. 5 Effects of ASD on the pathophysiological indices of BALF and serum in asthmatic mice. **(A)** Total cells, **(B)** eosinophils, **(C)** macrophages, **(D)** neutrophils, **(E)** TNF- α in BALF, **(F)** IL-6 in BALF, **(G)** IL-4 in BALF, **(H)** IL-13 in BALF, and **(I)** OVA-specific immunoglobulin (Ig) E in serum. NC, normal control; ovalbumin (OVA), Asthma model + PBS intranasal instillation; OVA + ASD10, 20, and 40, Asthma model + ASD (10, 20, and 40 mg/kg, respectively) intranasal instillation ($n=7$). ^{##}, versus NC, $p < 0.01$. ^{**}, versus OVA, $p < 0.05$ and < 0.01 , respectively

portion smaller than 2.5 μm . The elemental composition of ASD, with a high percentage of silica (43.4%) and oxygen (48.82%), is consistent with previous studies on desert dust particles, which are primarily composed of silicate minerals [21]. The presence of aluminum (4.73%) further suggests that ASD may possess oxidative properties, which could be relevant for assessing its potential toxicity and role in respiratory diseases [8]. The zeta potential of -32.48 mV indicates that the particles are stable in suspension, which is an important factor for understanding

how ASD may remain airborne for extended periods, potentially increasing exposure risk. These findings align with previous research indicating that particles of similar size and composition can penetrate deeply into the respiratory system, potentially leading to chronic health effects such as inflammation and oxidative stress [22, 23].

Exposure to ASD was harmful to the respiratory tract through the enhancement of release of inflammatory cytokines [24]. In particular, IL-6, a well-known inflammatory marker, activates the immune system in response

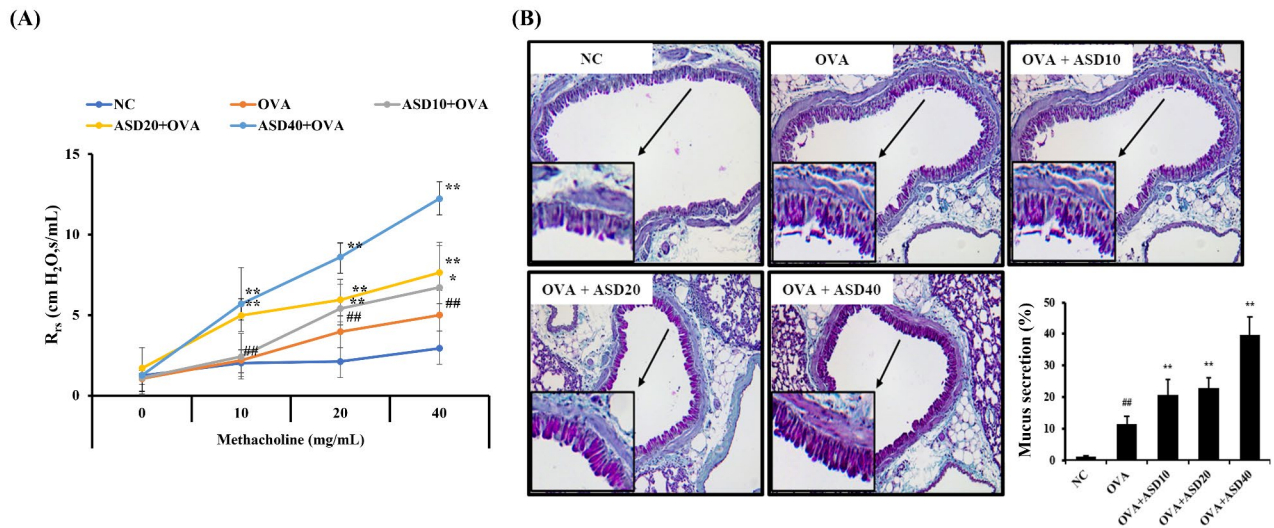


Fig. 6 Effects of ASD on airway hyperresponsiveness (AHR) and mucus production in asthmatic mice. **(A)** Airway hyperresponsiveness, **(B)** figure of mucus production and quantitative analysis. NC, normal control; OVA, Asthma model+PBS intranasal instillation; OVA+ASD10, 20, and 40, Asthma model+ASD (10, 20, and 40 mg/kg, respectively) intranasal instillation ($n=7$). ##, versus NC, $p<0.01$. **, versus OVA, $p<0.01$

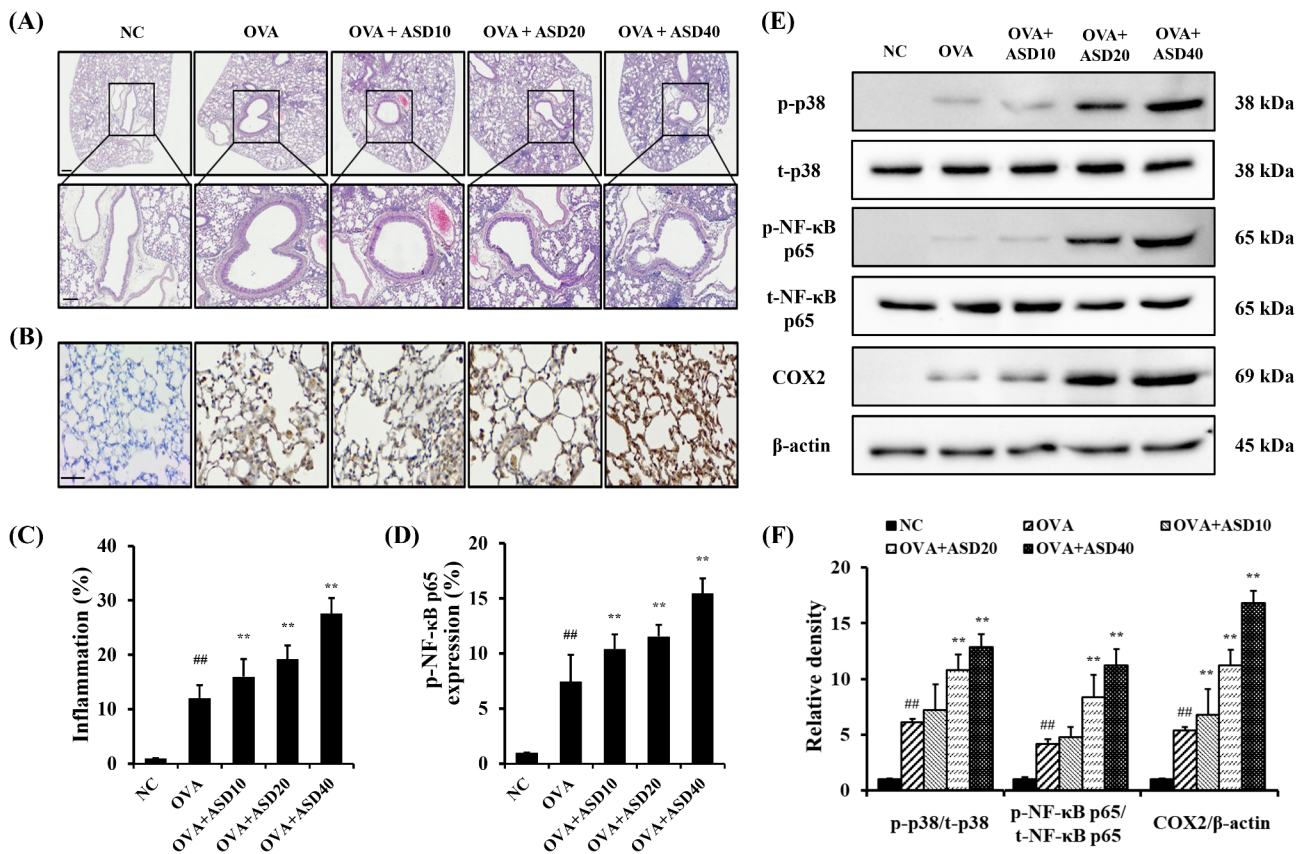


Fig. 7 Effects of ASD on pulmonary inflammation and p-NF-κB expression in asthmatic mice. **(A)** Representative figure of H&E staining, **(B)** representative figure of IHC (p-NF-κB p65), **(C)** quantitative analysis of inflammation, **(D)** quantitative analysis of p-NF-κB p65 expression, **(E)** representative figure of Western blot, **(F)** quantitative analysis of each protein. NC, normal control; OVA, Asthma model+PBS intranasal instillation; OVA+ASD10, 20, and 40, Asthma model+ASD (10, 20, and 40 mg/kg, respectively) intranasal instillation ($n=7$). ##, versus NC, $p<0.01$. **, versus OVA, $p<0.01$

to specific irritants, leading to increased neutrophil production in the bone marrow. Consequently, exposure to ASD induces the accumulation of neutrophils at damaged lesions [25–27]. Accumulated neutrophils consistently induced the infiltration of inflammatory cells into damaged lesions via their chemoattractant property and damaged normal cellular structures via the production various proteolytic enzymes caused by degranulation [28, 29]. In the present study, exposure to ASD elevated the number of inflammatory cells and cytokines in the BALF, similar to the effects observed with exposure to silica dioxide and aluminum oxide nanoparticles [30, 31], which was confirmed by histological analysis.

Allergic asthma is a complex pulmonary inflammatory disorder that AHR, pulmonary inflammation and mucus secretion [16]. Among various inflammatory cells, eosinophils, neutrophils, and macrophages are activated by many allergens and then release inflammatory mediators by degranulation. Type 2 cytokines, including IL-4, -5, and -13, are involved in promoting B cell class switching to produce IgE, recruiting eosinophils to the airways, stimulating goblet cell hyperplasia, and increasing airway smooth muscle contractility [32]. Recently, with an increase in air pollution, the degree of allergic asthma has increased and poses a serious threat to human health [12]. In present study, ASD exposure in OVA-inhaled mice elevated the asthmatic index including cytokines, the number of inflammatory cells, and allergen specific IgE compared with OVA-exposed mice, which is consistent with the evidence of histological examination, showing pulmonary inflammatory responses and mucus production. These results are consistent with a previous study [12]. Like the results of the toxicity study of ASD, when ASD was exposed to asthmatic animals, there was a considerable elevation in inflammatory cytokines and numbers of neutrophils and eosinophils in the BALF. In a murine model of ovalbumin-induced allergic asthma, co-exposure to silica dioxide nanoparticles and aluminum oxide nanoparticles exacerbated allergic airway inflammation associated with an increased type 2 immune response [8, 33]. These evidence indicated that ASD exposure may aggravate inflammatory responses induced by allergic asthma.

NF- κ B and mitogen-activated protein kinase (MAPK) are central mediators in the progression of inflammatory responses during the progression of various diseases [11, 34]. NF- κ B p65 is phosphorylated via a specific stimulus and is then translocated into the nucleus, where it eventually causes the transcription of numerous inflammatory factors such as COX2, TNF- α , IL-1 β , and -6. The p38 MAPK plays a pivotal role in inflammation, participating in both innate and adaptive immune responses by regulating the various inflammatory mediators [35]. NF- κ B recruitment is regulated by p38 MAPK

by increasing the accessibility of NF- κ B binding sites in NF- κ B-dependent promoters [36]. It has also been shown that p38 MAPK and NF- κ B regulate the level of COX2 expression in airway myocytes [37]. Due to this series of reactions, an inflammatory response develops in lesions exposed to the specific stimulus. In this study, ASD exposure induced the phosphorylation of NF- κ B p65 in pulmonary tissues, which was accompanied by an increase in inflammatory cell accumulation into pulmonary tissues. This evidence indicated that pulmonary inflammatory responses caused by ASD exposure was associated with the p-NF- κ B p65. Several studies have reported that PM exposure induces airway inflammation mediated by p-NF- κ B pathway [22, 38]. In addition, NF- κ B p65 appears to be important in allergic asthma [13]. The expression of p-NF- κ B was enhanced in bronchial biopsies and sputum from asthmatic patients and a murine model of allergic asthma, compared to controls [39]. However, NF- κ B knockout mice exhibited a reduction in airway inflammation responses to allergen exposure via a decrease in the releases of cytokines and chemokines [40]. In present study, ASD exposure to asthmatic mice markedly elevated the expression of p-NF- κ B p65 in pulmonary tissues compared with asthmatic mice alone, which was accompanied by the elevation of the number of inflammatory cells, cytokine, AHR, and mucus production. These results indicated that ASD exposure may exacerbate the degree of allergic asthma via the phosphorylation of NF- κ B expression.

Conclusions

Exposure to ASD leads to pulmonary inflammatory responses, including an elevation of inflammatory cell infiltration and cytokine production. These reactions were exacerbated in OVA-inhaled asthmatic mice and were involved with the phosphorylation of NF- κ B expression. Therefore, our results indicated that exposure to ASD may be an important risk factor for patients with allergic asthma.

Abbreviations

AHR	Airway hyperresponsiveness
ASD	Asian sand dust
BALF	Bronchoalveolar lavage fluid
COX2	Cyclooxygenase 2
ELISA	Enzyme-linked immunosorbent assay
Ig	Immunoglobulin
IL	Interleukin
MAPK	Mitogen-activated protein kinase
NC	Normal control
NF- κ B	Nuclear factor-kappa B
OVA	Ovalbumin
PBS	Phosphate-buffered saline
PM	Particulate matter
SEM	Scanning electron microscopy
TBST	Tris-buffered saline containing Tween 20
TEM	Transmission electron microscopy
TNF	Tumor necrosis factor

Supplementary Information

The online version contains supplementary material available at <https://doi.org/10.1186/s42826-025-00243-9>.

Supplementary Material 1

Acknowledgements

Not applicable.

Author contributions

Conceptualization: Kim SH, Shin IS; Methodology: Lee SJ, Pak SW; Formal analysis: Kim WI, Park SH, Cho YK, Kim TW, Ko JW, KIM IH; Investigation: Lee SJ; Data curation: Pak SW; Writing—original draft: Lee SJ; Writing—review and editing: Kim JC, Kim SH, Shin IS; Supervision: Shin IS; Funding acquisition: Kim JS, Shin IS. All authors have read and agreed to the published version of the manuscript.

Funding

This work was supported by the national Research Foundation of Korea granted by Korea Government (NRF-2020R1A4A1019395, RS-2022-NR069617 and RS-2023-00219517).

Data availability

The datasets used and/or analyzed during the current study are available from the corresponding author upon reasonable request.

Declarations

Ethics approval and consent to participate

Approval of animal studies was in accordance with the ethical guidelines and regulations established by the Institutional Animal Care and Use Committee of Chonnam National University (IACUC) carried out under approval numbers CNU IACUC-YB-R-2020-93 and CNU IACUC-YB-R-2021-36. Since this study did not involve human participants or clinical trials, ethical approval and consent to participate were not required.

Consent for publication

Not applicable.

Competing interests

The authors declare no conflicts of interest.

Received: 27 November 2024 / Revised: 23 March 2025 / Accepted: 12 April 2025

Published online: 09 May 2025

References

1. Tan S-C, Li J, Che H, Chen B, Wang H. Transport of East Asian dust storms to the marginal seas of China and the Southern North Pacific in spring 2010. *Atmos Environ*. 2017;148:316–28.
2. Kim WI, Lim JO, Pak SW, Lee SJ, Shin IS, Moon C, et al. Exposure to China dust exacerbates testicular toxicity induced by cyclophosphamide in mice. *Toxicol Res*. 2023;39:115–25.
3. Kim K, Kim SD, Shin TH, Bae CS, Ahn T, Shin SS, et al. Respiratory and systemic toxicity of inhaled artificial Asian sand dust in pigs. *Life (Basel)*. 2021;11(1):25.
4. Roy D, Kim J, Lee M, Park J. Adverse impacts of Asian dust events on human health and the environment—A probabilistic risk assessment study on particulate matter-bound metals and bacteria in Seoul, South Korea. *Sci Total Environ*. 2023;875:162637.
5. Requena-Mullor M, Alarcón-Rodríguez R, Parrón-Carreño T, Martínez-López JJ, Lozano-Paniagua D, Hernández AF. Association between crystalline silica dust exposure and silicosis development in artificial stone workers. *Int J Environ Res Public Health*. 2021;18(11):5625.
6. Nakao M, Yamauchi K, Mitsuma S, Odaira T, Obata H, Chijimatsu Y, et al. Associations of ambient air pollutant concentrations with respiratory symptoms and perceived health status in Japanese adults with and without chronic respiratory diseases: A panel study. *J Prev Med Public Health*. 2019;52:416–26.
7. Tong H, Cong S, Fang LW, Fan J, Wang N, Zhao QQ, et al. [Performance of pulmonary function test in people aged 40 years and above in China, 2019–2020]. *Zhonghua Liu Xing Bing Xue Za Zhi*. 2023;44:727–34.
8. Lim JO, Kim WI, Pak SW, Lee SJ, Park SH, Shin IS, et al. Toll-like receptor 4 is a key regulator of asthma exacerbation caused by aluminum oxide nanoparticles via regulation of NF- κ B phosphorylation. *J Hazard Mater*. 2023;448:130884.
9. Tao X, Li J, He J, Jiang Y, Liu C, Cao W, et al. Pinella ternata (Thunb.) Breit. Attenuates the allergic airway inflammation of cold asthma via inhibiting the activation of TLR4-mediated NF- κ B and NLRP3 signaling pathway. *J Ethnopharmacol*. 2023;315:116720.
10. Park JW, Kwon OK, Ryu HW, Paik JH, Paryanto I, Yuniato P, et al. Anti-inflammatory effects of Passiflora foetida L. in LPS-stimulated RAW264.7 macrophages. *Int J Mol Med*. 2018;41:3709–16.
11. Giridharan S, Srinivasan M. Mechanisms of NF- κ B p65 and strategies for therapeutic manipulation. *J Inflamm Res*. 2018;11:407–19.
12. Kim HJ, Song JY, Park TI, Choi WS, Kim JH, Kwon OS, et al. The effects of BRL-50481 on ovalbumin-induced asthmatic lung inflammation exacerbated by co-exposure to Asian sand dust in the murine model. *Arch Pharm Res*. 2022;45:51–62.
13. Charokopos N, Apostolopoulos N, Kalapodi M, Leotsinidis M, Karamanos N, Mouzaki A. Bronchial asthma, chronic obstructive pulmonary disease and NF-kappaB. *Curr Med Chem*. 2009;16:867–83.
14. Babu KS, Davies DE, Holgate ST. Role of tumor necrosis factor alpha in asthma. *Immunol Allergy Clin North Am*. 2004;24:583–97. v-vi.
15. Lee SJ, Pak SW, Kim WI, Park SH, Cho YK, Ko JW, et al. Silibinin suppresses inflammatory responses induced by exposure to Asian sand dust. *Antioxid (Basel)*. 2024;13(10):1187.
16. Pak S-W, Lee AY, Seo Y-S, Lee S-J, Kim W-I, Shin D-H, et al. Anti-asthmatic effects of Phlomis umbrosa Turczaninow using ovalbumin induced asthma murine model and network Pharmacology analysis. *Biomed Pharmacother*. 2022;145:112410.
17. Sadakane K, Ichinose T, Nishikawa M. Effects of co-exposure of lipopolysaccharide and β -glucan (Zymosan A) in exacerbating murine allergic asthma associated with Asian sand dust. *J Appl Toxicol*. 2019;39:672–84.
18. Sadakane K, Ichinose T, Maki T, Nishikawa M. Co-exposure of peptidoglycan and heat-inactivated Asian sand dust exacerbates ovalbumin-induced allergic airway inflammation in mice. *Inhal Toxicol*. 2022;34:231–43.
19. Nakao M, Ishihara Y, Kim CH, Hyun IG. The impact of air pollution, including Asian sand dust, on respiratory symptoms and Health-related quality of life in outpatients with chronic respiratory disease in Korea: A panel study. *J Prev Med Public Health*. 2018;51:130–9.
20. Valavanidis A, Fiotakis K, Vlachogianni T. Airborne particulate matter and human health: toxicological assessment and importance of size and composition of particles for oxidative damage and carcinogenic mechanisms. *J Environ Sci Health C Environ Carcinog Ecotoxicol Rev*. 2008;26:339–62.
21. Ichinose T, Yoshida S, Sadakane K, Takano H, Yanagisawa R, Inoue K, et al. Effects of Asian sand dust, Arizona sand dust, amorphous silica and aluminum oxide on allergic inflammation in the murine lung. *Inhal Toxicol*. 2008;20:685–94.
22. Ha JH, Lee BW, Yi DH, Lee SJ, Kim WI, Pak SW, et al. Particulate matter-mediated oxidative stress induces airway inflammation and pulmonary dysfunction through TXNIP/NF- κ B and modulation of the SIRT1-mediated p53 and TGF- β /Smad3 pathways in mice. *Food Chem Toxicol*. 2024;183:114201.
23. Pak SW, Kim WI, Lee SJ, Park SH, Cho YK, Kim JS, et al. TXNIP regulates pulmonary inflammation induced by Asian sand dust. *Redox Biol*. 2024;78:103421.
24. Yang HW, Park JH, Shin JM, Lee HM, Park IH. Asian sand dust upregulates IL-6 and IL-8 via ROS, JNK, ERK, and CREB signaling in human nasal fibroblasts. *Am J Rhinol Allergy*. 2020;34:249–61.
25. Almeida CR, Lima JF, Machado MR, Alves JV, Couto AES, Campos LCB, et al. Inhibition of IL-6 signaling prevents serum-induced umbilical cord artery dysfunction from patients with severe COVID-19. *Am J Physiol Regul Integr Comp Physiol*. 2023;324(4):R435–45.
26. Garth J, Barnes JW, Krick S. Targeting cytokines as evolving treatment strategies in chronic inflammatory airway diseases. *Int J Mol Sci*. 2018;19(11):3402.
27. Oz-Tuncer G, Olgunturk R, Pektas A, Cilsal E, Kula S, Oguz DA, et al. The role of inflammatory biomarkers in CHD-associated pulmonary hypertension in children. *Cardiol Young*. 2017;27:255–60.
28. El Rayes T, Catena R, Lee S, Stawowczyk M, Joshi N, Fischbach C, et al. Lung inflammation promotes metastasis through neutrophil protease-mediated degradation of Tsp-1. *Proc Natl Acad Sci U S A*. 2015;112:16000–5.

29. Tsai YF, Yu HP, Chung PJ, Leu YL, Kuo LM, Chen CY, et al. Osthol attenuates neutrophilic oxidative stress and hemorrhagic shock-induced lung injury via Inhibition of phosphodiesterase 4. *Free Radic Biol Med*. 2015;89:387–400.
30. Kwon J-T, Seo G-B, Lee M, Kim H-M, Shim I, Jo E, et al. [Pulmonary toxicity assessment of aluminum oxide nanoparticles via nasal instillation exposure]. *J Environ Health Sci*. 2013;39:48–55.
31. Lim J-O, Ko J-W, Jung T-Y, Kim W-I, Pak S-W, Shin I-S, et al. Pulmonary inflammation caused by silica dioxide nanoparticles in mice via TXNIP/NLRP3 signaling pathway. *Mol Cell Toxicol*. 2020;16:245–52.
32. Nur Husna SM, Md Shukri N, Mohd Ashari NS, Wong KK. IL-4/IL-13 axis as therapeutic targets in allergic rhinitis and asthma. *PeerJ*. 2022;10:e13444.
33. Ko J-W, Shin N-R, Je-Oh L, Jung T-Y, Moon C, Kim T-W, et al. Silica dioxide nanoparticles aggravate airway inflammation in an asthmatic mouse model via NLRP3 inflammasome activation. *Regul Toxicol Pharmacol*. 2020;112:104618.
34. Saklatvala J. The p38 MAP kinase pathway as a therapeutic target in inflammatory disease. *Curr Opin Pharmacol*. 2004;4:372–7.
35. Schieven GL. The p38alpha kinase plays a central role in inflammation. *Curr Top Med Chem*. 2009;9:1038–48.
36. Saccani S, Pantano S, Natoli G. p38-Dependent marking of inflammatory genes for increased NF-kappa B recruitment. *Nat Immunol*. 2002;3:69–75.
37. Singer CA, Baker KJ, McCaffrey A, AuCoin DP, Dechert MA, Gerthoffer WT. p38 MAPK and NF-kappaB mediate COX-2 expression in human airway myocytes. *Am J Physiol Lung Cell Mol Physiol*. 2003;285:L1087–98.
38. Cattani-Cavaliere I, Valenca SS, Lanzetti M, Carvalho GMC, Zin WA, Monte-Alto-Costa A, et al. Acute exposure to Diesel-Biodiesel particulate matter promotes murine lung oxidative stress by Nrf2/HO-1 and inflammation through the NF-kB/TNF- α pathways. *Inflammation*. 2019;42:526–37.
39. Kelly C, Shields MD, Elborn JS, Schock BC. A20 regulation of nuclear factor- κ B: perspectives for inflammatory lung disease. *Am J Respir Cell Mol Biol*. 2011;44:743–8.
40. Edwards MR, Bartlett NW, Clarke D, Birrell M, Belvisi M, Johnston SL. Targeting the NF-kappaB pathway in asthma and chronic obstructive pulmonary disease. *Pharmacol Ther*. 2009;121:1–13.

Publisher's note

Springer Nature remains neutral with regard to jurisdictional claims in published maps and institutional affiliations.